

# p53 Unfolding Detected by CD but Not by Tryptophan Fluorescence<sup>1</sup>

Nicole Magnasco Nichols and Kathleen Shive Matthews<sup>2</sup>

*Department of Biochemistry & Cell Biology, Rice University, MS102, Houston, Texas 77005*

Received August 30, 2001

**Full-length human p53 protein was examined using tryptophan fluorescence and circular dichroism spectroscopy (CD) to monitor unfolding. No significant alteration in tryptophan fluorescence for the tetrameric protein was detectable over a wide range of either urea or guanidine hydrochloride concentrations, in contrast to results with the isolated DNA binding domain [Bullock *et al.* (1997) *Proc. Natl. Acad. Sci. USA* 94, 14338]. Under similar denaturant conditions, CD demonstrated significant protein unfolding for the full-length wild-type protein, with increased apparent structure loss compared to that detected during thermal denaturation [Nichols and Matthews (2001) *Biochemistry* 40, 3847]. Examination of X-ray structures containing two of the four tryptophan residues of a p53 monomer suggested local environments consistent with quenched fluorophores. Exploration of p53 fluorescence using potassium iodide as a quencher confirmed that these fluorophores are already substantially quenched in the native structure, and this quenching is not relieved during protein unfolding.** © 2001 Academic Press

**Key Words:** p53 protein; fluorescence; stability; unfolding; quenching; circular dichroism.

The ability of the homotetrameric tumor suppressor protein p53 to protect against uncontrolled cellular growth depends on its ability to recognize cognate dsDNA sequences, as reflected in the loss of this activity in a large percentage of human tumors (reviewed in 1, 2). Low cellular levels, maintained through MDM2-mediated ubiquitination and associated degradation, ensure that p53 action is limited under normal condi-

tions (reviewed in 3, 4). In response to cellular stress, p53 degradation is decreased, with a consequent increase in p53 levels, and posttranslational modifications occur that further affect degradation and alter functional properties of p53 (reviewed in 3–8).

Each full-length p53 monomer contains four tryptophans, all located in the N-terminal half of the protein (Fig. 1) (9, 10). Three of the tryptophan residues are in the N-terminal transactivation and SH2 signaling domains, whereas the remaining tryptophan is located in the DNA binding domain (9, 10) and serves as the signal for core domain unfolding analysis (11). Tryptophan fluorescence is highly sensitive to surrounding environment and can be used to monitor structural alterations in response to protein unfolding (12). Chemically induced unfolding of the monomeric core domain of p53 can be monitored by fluorescence of the sole tryptophan at position 146 in this fragment (11). The core domain unfolding process is reversible and occurs at relatively low denaturant concentrations (11). A contrasting view of the core domain within the full-length tetrameric protein is provided by monitoring loss of secondary structure using circular dichroism (CD) spectroscopy as a function of temperature (13).  $\beta$ -Sheet (corresponding to the core DNA binding domain) and  $\alpha$ -helical structures as well as the DNA binding function of isolated full-length p53 protein exhibit significant thermal stability (13). Because chemical and thermal unfolding often occur via distinct pathways and intermediates, these methods can provide complementary information (14). To explore the differences observed between the full-length, tetrameric p53 protein and the monomeric core DNA binding domain, we have examined chemically induced unfolding of the full-length protein using both fluorescence and CD spectroscopy. Interestingly, we find no effect on tryptophan fluorescence for the full-length protein even at high denaturant concentrations. The tryptophan residues in the native p53 protein are found to be highly quenched and are unsusceptible to further quenching by iodide. Thus, the indole side chains are ineffective tools for monitoring structural

<sup>1</sup> This work was supported by grants from the G. Harold and Leila Y. Mathers Foundation and from the Robert A. Welch Foundation (C-576) to K.S.M. N.M.N. was supported by an NIH Molecular Biophysics Training Grant (GM-08280). Spectroscopic facilities were provided by the Keck Center for Computational Biology and the Lucille P. Markey Charitable Trust.

<sup>2</sup> To whom correspondence and reprint requests should be addressed. Fax: 713-348-6149. E-mail: ksm@rice.edu.

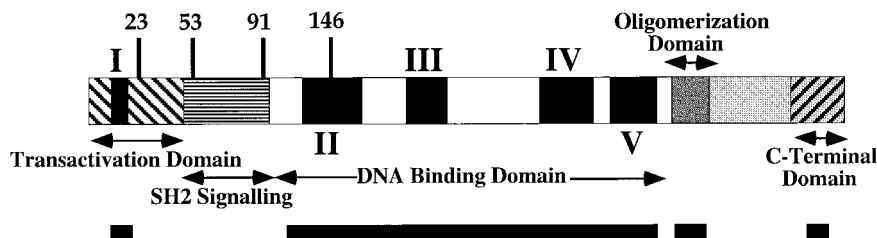


**FIG. 1.** Location of tryptophan residues on the linear amino acid sequence of p53. Vertical bars represent tryptophan locations and corresponding amino acid residue numbers (9, 10). Filled regions identified by Roman numerals indicate highly conserved regions, and functions for specific domains of the protein are labeled (reviewed in 2, 4, 5). Bars below the sequence indicate regions for which structures have been determined (16, 17, 19, 20). Trp146 is the only tryptophan located outside of the N-terminal activation/SH2 signaling domain in conserved region II of the core DNA binding domain.

integrity in the full-length protein. In contrast, CD spectroscopic measurements indicate substantial alterations in secondary structure in response to guanidine-HCl (GuHCl).

## MATERIALS AND METHODS

**Expression and purification of p53 protein.** Cell growth and protein purification were performed as described previously (13). p53 protein eluted from the final phosphocellulose column approximately midway through a 0.2–0.5 M KPB (potassium phosphate buffer, pH 7.5, 5 mM DTT, 10% (v/v) glycerol, 5% (w/v) glucose) gradient. Protein purity was determined by SDS-PAGE analysis and densitometry of the stained protein bands and ranged from ~80 to 90% per preparation.

**Chemical denaturants.** Stock solutions of guanidine hydrochloride (GuHCl) and urea were made from ultra-pure chemicals (Fluka) in buffer stocks at 2- to 5-fold final concentration. Concentration was determined after dilution to final concentration and filtration according to refractive index measurements using the following equations:

$$M_{\text{GuHCl}} = 57.147(\Delta N) + 38.68(\Delta N^2) - 91.60(\Delta N^3) \quad [1]$$

$$M_{\text{urea}} = 117.66(\Delta N) + 29.753(\Delta N^2) + 185.56(\Delta N^3), \quad [2]$$

where  $\Delta N$  is the difference in the index of refraction between the stock GuHCl or urea sample and the corresponding buffer at the sodium D line (14). Stock solutions of urea were made fresh daily to prevent the formation of cyanate ions (14).

**Fluorescence measurements.** Spectra were measured on either a modular SLM Aminco fluorometer or an SLM Amino-Bowman Series 2 luminescence spectrometer. Protein concentration was  $5 \times 10^{-7}$  M<sub>tet</sub> in ~0.33 M potassium phosphate buffer, pH 7.5, and samples were scanned at room temperature from 310 to 370 nm at 2 nm/s with an excitation wavelength of 285 nm. A Corning filter 7-54 was used in the excitation pathway to allow light of wavelengths 240 through 420 nm to pass to the sample. For comparative studies with *N*-acetyl-L-tryptophanamide, p53 protein concentration was converted to molar tryptophan concentrations. For chemical denaturation measurements, samples of  $3 \times 10^{-7}$  M<sub>tet</sub> p53 protein were allowed to incubate in varying concentrations of denaturant from 2 to 24 h before spectra were collected from 310 to 370 nm at room temperature. Varying the potassium phosphate concentration for the measurements from 0.1 to 0.35 M did not alter results obtained.

**Iodide quenching.** Potassium iodide quenching experiments were performed on a modular SLM Aminco Fluorometer fitted with a stirring motor. A stock solution of 5 M KI, 1 mM sodium thiosulfate

(to prevent I<sub>2</sub> formation) was made to allow very small volume additions (5  $\mu$ l into 1.0 ml protein sample) via Hamilton syringe, after which the solution was mixed for 25 s before spectra were collected. The experiment was repeated with buffer additions to a protein solution to provide correction values for noniodide sources of quenching. The Stern-Volmer constant,  $K_{SV}$ , was determined from these data (12).

**Circular dichroism measurements.** Data were collected on an AVIV Model 62A DS circular dichroism spectrometer. Circular dichroism intensity for wild-type p53 was monitored at 218 nm at 22°C at various concentrations of urea. For GuHCl experiments, the CD spectrometer was fitted with a stir motor and a double Hamilton syringe pump titrator accessory. Unfolded protein stock solutions were generated by incubation of the protein for 30 min in the presence of denaturant. Incubations from 10 min to 4 h indicated that unfolding occurs within 10 min of denaturant addition, and 30 min was selected for experimental measurements. p53 protein [0.1 mg/ml ( $8.0 \times 10^{-7}$  M<sub>tet</sub>) in 0.4 M KPB, 0 M GuHCl] was monitored at 218 nm in the sample compartment in a 1  $\times$  1-cm quartz cuvette while a stock of unfolded protein [0.1 mg/ml ( $8.0 \times 10^{-7}$  M<sub>tet</sub>) in 0.4 M KPB, 5 M GuHCl] was controlled by the syringe pump system. Samples were also examined at ~0.3 M KPB with no alteration in results observed. Reverse experiments were conducted to monitor the refolding of p53 to ensure reversibility, and data points from both folding and unfolding experiments overlapped. Measurements at each denaturant concentration were averaged over a 10-s collection window. Identical results were achieved by mixing the samples for various times (120–360 s) after each denaturant addition, verifying that data were collected under equilibrium conditions.

## RESULTS

**Tryptophan fluorescence.** To assess the relative solvent exposure and chemical environment of the tryptophans in p53, the protein fluorescence spectrum was compared to that for *N*-acetyltryptophanamide at a comparable molar concentration of tryptophan fluorophores (Fig. 2). *N*-Acetyltryptophanamide can be used to approximate the spectrum of a protein tryptophan fluorophore fully exposed to solvent, because its fluorophore is fully exposed in solution and the amino and carboxyl groups are blocked. The intensity of the spectrum for p53 was substantially diminished compared to *N*-acetyltryptophanamide, suggesting substantial quenching of all four tryptophans in the native environment of p53.

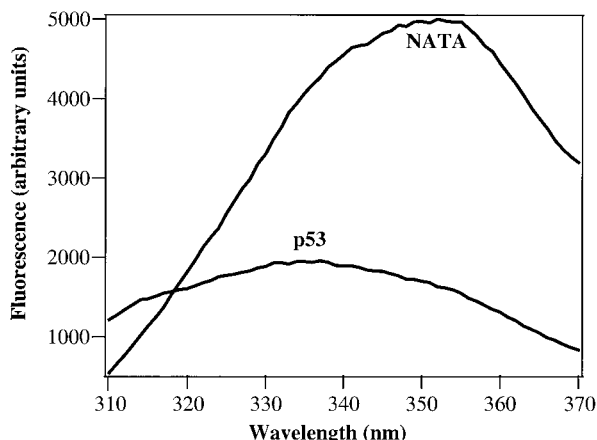


**FIG. 2.** Fluorescence spectra for wild-type p53 protein and *N*-acetyltryptophanamide at the same molar tryptophan concentration. *N*-Acetyltryptophanamide is commonly used as a tryptophan fluorescence standard that exhibits a wavelength of maximum emission and quantum yield characteristic of a solvent-exposed tryptophan (~350 nm). Samples were excited at 285 nm, and emission spectra were collected from 310 to 370 nm at 2 nm/s.

**Iodide quenching of tryptophan fluorescence.** p53 tryptophan accessibility was probed by potassium iodide quenching experiments to determine whether the fluorescence of any of the four tryptophans of p53 could be decreased by collisional quenching. Iodide is a potent fluorescence quencher whose charge and large size prevents it from approaching tryptophans located within the hydrophobic core of a protein. Iodide quenching can therefore be correlated to the accessibility of the residues, providing information about their environment (12). Iodide quenching effectiveness is measured as the Stern-Volmer quenching constant,  $K_{SV}$ , where a  $K_{SV} \leq 0.2$  represents essentially no quenching (12). The Stern-Volmer constant derived from these experiments was  $0.15 \pm 0.11 \text{ M}^{-1}$ , indicating that none of the four tryptophans can be quenched effectively by KI.

**Chemical denaturation monitored by fluorescence.** Fluorescence of full-length p53 protein was examined as a function of chemical denaturant concentration. No significant change in fluorescence was observed for the full-length wild-type protein, even at concentrations of 6 M urea (Fig. 3A). Previous experiments with the isolated, monomeric DNA binding domain had demonstrated that ~2.7 M urea was sufficient to unfold 50% of this monomeric polypeptide at 25°C (11). GuHCl generally unfolds proteins at lower concentrations than urea and generates 50% unfolding of the DNA binding domain at 1.1 M at 10°C (15). This reagent was also employed in our fluorescence experiments, and up to 5 M GuHCl we observed no alteration in fluorescence signal (Fig. 3B). Samples were monitored for up to 24 h to exclude the possibility that slow unfolding kinetics were responsible for the unchanged fluores-

cence spectra. No alteration in the results was observed. Two possible explanations can account for the absence of any significant change in p53 fluorescence signal as a function of chemical denaturant. Either no significant change in tryptophan environment takes place in the intact protein, i.e., full-length, tetrameric p53 cannot be unfolded by high concentrations of urea or GuHCl, or there is a change in structure that the tryptophans do not report. Because of the different observations for the DNA binding domain in the isolated core polypeptide (11, 15) and the full-length protein (minimal fluorescence change at high denaturant concentrations as well as very high thermal stability) (13), circular dichroism was used to monitor response of secondary structure within the full-length protein to chemical denaturants.

**Circular dichroism measurements of unfolding.** CD spectra were collected at 22°C as a function of both urea and GuHCl concentrations to assess the folded state of p53 protein. The stability of p53 tetramer is reflected in the low level of structure disruption observed up to 4 M urea (Fig. 4). Clearly the full-length protein stability exceeds that observed for the isolated DNA binding domain which is 50% unfolded at 2.7 M urea at 25°C (11). Higher concentrations of urea were

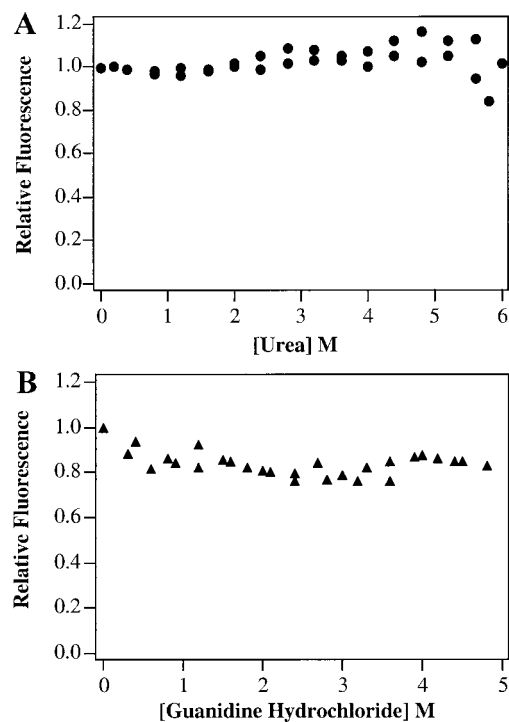


**FIG. 3.** p53 tryptophan fluorescence as a function of denaturant concentration. Relative fluorescence intensity of wild-type p53 reported at 340 nm was measured as a function of (A) urea or (B) GuHCl concentration as described under Materials and Methods. Relative fluorescence was measured by normalizing the fluorescence intensity at 340 nm to that displayed by a protein sample in the absence of denaturant.

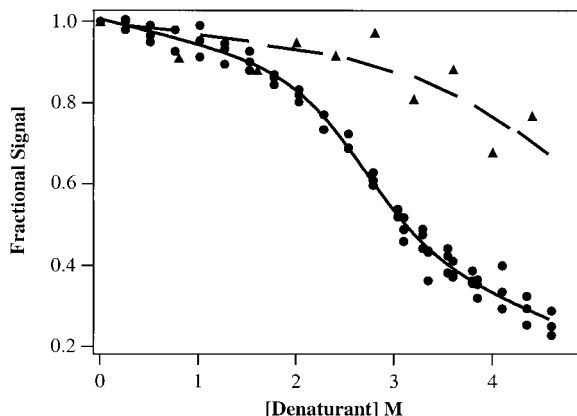


**FIG. 4.** Circular dichroism intensity as a function of denaturant. Signal was monitored at 218 nm at 22°C and reported as a fractional signal relative to the intensity observed in the absence of denaturant. Data from duplicate experiments for urea (triangles) and triplicate experiments for GuHCl (circles) are shown. Data from renaturation experiments for GuHCl were similar to those collected from denaturation experiments. These data are included in the figure and were designed to overlap denaturation data points between 3 and 4 M GuHCl. Higher concentrations of GuHCl to achieve the lower plateau necessary for thermodynamic analysis could not be obtained due to experimental constraints.

precluded by limitations of protein concentration. GuHCl, which is a stronger chemical denaturant, was utilized to determine whether this compound could effect complete unfolding, and the spectral changes observed clearly reflect loss of  $\alpha$ -helical and  $\beta$ -sheet structure (13). Even at 4.8 M GuHCl, the protein did not appear to be completely unfolded, as reflected in the absence of a lower plateau in Fig. 4. Requisite buffer conditions and limitations on protein concentration that could be obtained prevented the use of higher denaturant concentrations. At 4.8 M GuHCl, approximately 30% of the starting structure signal remained. To ensure that slow unfolding was not responsible for the absence of complete denaturation, samples were monitored for a period of many hours. Equilibrium conditions were reached on the order of several minutes, well within the incubation times of the measurements. Renaturation experiments were conducted to verify the reversibility of protein unfolding, and results were identical to those from GuHCl denaturation experiments over the entire range investigated (Fig. 4).

## DISCUSSION

Monomeric DNA binding domains from tumor-derived p53 mutants have been reported to exhibit diminished stability that may account for their decreased DNA binding (11, 15). Determining the thermodynamics of full-length, tetrameric p53 folding has therefore gained importance. Significant thermal stability of both structure and function has been demon-

strated for the full-length p53 protein isolated without post-translational modifications from bacterial cells (13); however, the unfolding observed with increased temperature is irreversible, precluding thermodynamic analysis of this process. To initiate an exploration of thermodynamic parameters for the full-length, tetrameric p53 protein and establish baseline information on this system, we employed fluorescence spectroscopy to monitor protein unfolding. Fluorescence analysis was selected based on the success of this technique in monitoring monomeric p53 DNA binding domain unfolding (11, 15). Despite four potential fluorophores per monomer, comparable experiments with the full-length p53 protein gave extremely low fluorescence signal that was unaltered over a wide range of denaturant concentrations. Thus, comparable fluorescence behavior is not observed in the intact protein as for the DNA binding domain alone.

Iodide, which accesses exposed or only partially buried fluorophores, was used to determine whether tryptophans in full-length p53 protein were susceptible to additional quenching. Iodide did not elicit any additional diminution in the fluorescence signal for p53 protein. The absence of significant quenching in p53 could arise from either inaccessibility of tryptophan residues to the quencher or from intrinsic quenching of the tryptophan residues.

The environments of two of the four tryptophans of p53 can be examined using the X-ray structures of p53 domains (16, 17). Trp146 is located in the N-terminal end of the DNA binding core domain in a  $\beta$ -sheet in conserved region II (Fig. 1). Residues surrounding Trp146 include Arg110, Asp228, Cys229, and Gln144 (17), all capable of quenching tryptophan fluorescence (12). The location of Trp146 in this charged pocket accounts for its low fluorescence, but this arrangement does not account for differential fluorescence behavior for Trp146 between the isolated DNA binding domain and the intact protein. Additional interactions of the N- and C-terminal regions within the full-length protein as well as contact between subunits may alter substantially the environment to which this tryptophan is exposed in the native and partially unfolded states.

Three of the four tryptophans of p53 are located in the loosely structured N-terminal domain (18). The environment of one of these, Trp23, can be inferred from the crystallographic structure of a small, N-terminal peptide that was reported to form a complex with an MDM2 fragment (16). Residues Phe19, Leu26, Pro27 combine with Trp23 to form a hydrophobic surface that is recognized by MDM2. When MDM2 is not bound to p53, the helical structure is unlikely to form, and these residues are presumably solvent exposed. Such an environment for Trp23 would also be consistent with low fluorescence intensity. Further work will be necessary to establish unequivocally the basis for the diminished fluorescence quantum yield for

the remaining p53 tryptophans, but their position in the less structured N-terminal domain suggests that solvent exposure may also account for their behavior.

To confirm that the p53 protein unfolds over the range of denaturant concentrations where no alteration in fluorescence could be detected, circular dichroism spectroscopy was utilized to monitor the secondary structure of the protein. These experiments demonstrate that full-length wild-type p53 protein is not substantially unfolded by urea in the concentrations accessible experimentally, in contrast to the isolated core domain (11). However, the full-length protein can be significantly unfolded (loss of ~70% signal) by the stronger denaturant, GuHCl. Denaturation of full-length p53 protein with GuHCl is a reversible and relatively rapid kinetic process that is complete within 1–2 min. However, the inability to attain a lower plateau, coupled with lack of knowledge regarding intermediate structures, precludes thermodynamic analysis of these data.

Differences in fluorescence during denaturation of the isolated, monomeric core DNA binding domain versus the full-length tetrameric protein suggest significant effects of other domains and assembly on unfolding for p53 protein. In addition to enhancing stability, the native state of the protein may engage a variety of intratetrameric interactions that result in quenching of intrinsic tryptophan fluorescence. Since no detectable change in fluorescence is observed over a range of denaturant concentrations in which substantial changes in secondary structure are observed by CD, the quenched state of the tryptophan fluorophores must be maintained throughout the course of the unfolding reaction even as disruption of secondary structure occurs. Further study is required to decipher the origins of these effects and to generate a complete thermodynamic analysis of unfolding processes for this complex and interesting protein.

## REFERENCES

1. Tominaga, O., Hamelin, R., Remvikos, Y., Salmon, R. J., and Thomas, G. (1992) p53 from basic research to clinical applications. *Crit. Rev. Oncogen.* **3**, 257–282.
2. Donehower, L. A., and Bradley, A. (1993) The tumor suppressor p53. *Biochim. Biophys. Acta* **1155**, 181–205.
3. Prives, C. (1998) Signaling to p53: Breaking the MDM2-p53 circuit. *Cell* **95**, 5–8.
4. Appella, E., and Anderson, C. W. (2000) Signaling to p53: Breaking the posttranslational modification code. *Pathol. Biol.* **48**, 227–245.
5. May, P., and May, E. (1999) Twenty years of p53 research: Structural and functional aspects of the p53 protein. *Oncogene* **18**, 7621–7636.
6. Jayaraman, L., and Prives, C. (1999) Covalent and noncovalent modifiers of the p53 protein. *Cell. Mol. Life Sci.* **55**, 76–87.
7. Meek, D. W. (1998) Multisite phosphorylation and the integration of stress signals at p53. *Cell. Signal.* **10**, 159–166.
8. Prives, C., and Hall, P. A. (1999) The p53 pathway. *J. Pathol.* **187**, 112–126.
9. Harlow, E., Williamson, N. M., Ralston, R., Helfman, D. M., and Adams, T. E. (1985) Molecular cloning and in vitro expression of a cDNA clone for human cellular tumor antigen p53. *Mol. Cell. Biol.* **5**, 1601–1610.
10. Zakut-Houri, R., Bienen-Tadmor, B., Givol, D., and Oren, M. (1985) Human p53 cellular tumor antigen: cDNA sequence and expression in COS cells. *EMBO J.* **4**, 1251–1255.
11. Bullock, A. N., Henckel, J., DeDecker, B. S., Johnson, C. M., Nikolova, P. V., Proctor, M. R., Lane, D. P., and Fersht, A. R. (1997) Thermodynamic stability of wild-type and mutant p53 core domain. *Proc. Natl. Acad. Sci. USA* **94**, 14338–14342.
12. Lakowicz, J. R. (1999) Principles of Fluorescence Spectroscopy, 2nd ed., Kluwer Academic/Plenum Publishers, New York.
13. Nichols, N. M., and Matthews, K. S. (2001) Protein–DNA binding correlates with structural thermostability for the full-length human p53 protein. *Biochemistry* **40**, 3847–3858.
14. Pace, C. N. (1986) Determination and analysis of urea and guanidine hydrochloride denaturation curves. *Methods Enzymol.* **131**, 266–280.
15. Bullock, A. N., Henckel, J., and Fersht, A. R. (2000) Quantitative analysis of residual folding and DNA binding in mutant p53 core domain: Definition of mutant states for rescue in cancer therapy. *Oncogene* **19**, 1245–1256.
16. Kussie, P. H., Gorina, S., Marechal, V., Elenbaas, B., Moreau, J., Levine, A. J., and Pavletich, N. P. (1996) Structure of the MDM2 oncoprotein bound to the p53 tumor suppressor transactivation domain. *Science* **274**, 948–953.
17. Cho, Y., Gorina, S., Jeffrey, P. D., and Pavletich, N. P. (1994) Crystal structure of a p53 tumor suppressor–DNA complex: Understanding tumorigenic mutations. *Science* **265**, 346–355.
18. Lee, H., Mok, K. H., Muhandiram, R., Park, K.-H., Suk, J.-E., Kim, D.-H., Chang, J., Sung, Y. C., Choi, K. Y., and Han, K.-H. (2000) Local structural elements in the mostly unstructured transcriptional activation domain of human p53. *J. Biol. Chem.* **275**, 29426–29432.
19. Rustandi, R. R., Baldisseri, D. M., and Weber, D. J. (2000) Structure of the negative regulatory domain of p53 bound to S100B( $\beta\beta$ ). *Nat. Struct. Biol.* **7**, 570–574.
20. Jeffrey, P. D., Gorina, S., and Pavletich, N. P. (1995) Crystal structure of the tetramerization domain of the p53 tumor suppressor at 1.7 angstroms. (1995) *Science* **267**, 1498–1502.